

# Accepted Manuscript

Repurposing Hsp90 inhibitors as antibiotics targeting histidine kinases

Chau D. Vo, Hanna L. Shebert, Shannon Zikovich, Rebecca A. Dryer, Tony P. Huang, Lindsey J. Moran, Juno Cho, Douglas R. Wassarman, Bryn E. Falahee, Peter D. Young, Garrick H. Gu, James F. Heintz, John W. Hammond, Taylor N. Jackvony, Thomas E. Frederick, Jimmy A. Blair

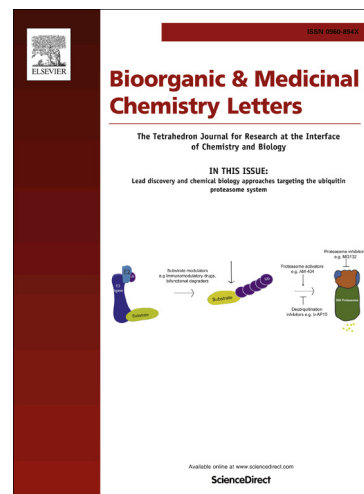
PII: S0960-894X(17)31030-2  
DOI: <https://doi.org/10.1016/j.bmcl.2017.10.036>  
Reference: BMCL 25365

To appear in: *Bioorganic & Medicinal Chemistry Letters*

Received Date: 26 June 2017  
Revised Date: 5 October 2017  
Accepted Date: 18 October 2017

Please cite this article as: Vo, C.D., Shebert, H.L., Zikovich, S., Dryer, R.A., Huang, T.P., Moran, L.J., Cho, J., Wassarman, D.R., Falahee, B.E., Young, P.D., Gu, G.H., Heintz, J.F., Hammond, J.W., Jackvony, T.N., Frederick, T.E., Blair, J.A., Repurposing Hsp90 inhibitors as antibiotics targeting histidine kinases, *Bioorganic & Medicinal Chemistry Letters* (2017), doi: <https://doi.org/10.1016/j.bmcl.2017.10.036>

This is a PDF file of an unedited manuscript that has been accepted for publication. As a service to our customers we are providing this early version of the manuscript. The manuscript will undergo copyediting, typesetting, and review of the resulting proof before it is published in its final form. Please note that during the production process errors may be discovered which could affect the content, and all legal disclaimers that apply to the journal pertain.



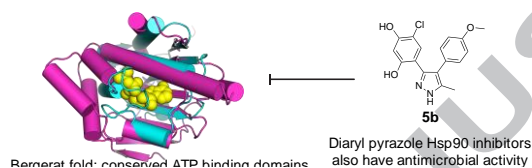
## Graphical Abstract

To create your abstract, type over the instructions in the template box below.  
Fonts or abstract dimensions should not be changed or altered.

### Repurposing Hsp90 inhibitors as antibiotics targeting histidine kinases

Leave this area blank for abstract info.

Chau D. Vo, Hanna L. Shebert, Shannon Zikovich, Rebecca A. Dryer, Tony P. Huang, Lindsey J. Moran, Juno Cho, Douglas R. Wassarman, Bryn E. Falahee, Peter D. Young, Garrick H. Gu, James F. Heini, John W. Hammond, Taylor N. Jackvony, Thomas E. Frederick, and Jimmy A. Blair





## Repurposing Hsp90 inhibitors as antibiotics targeting histidine kinases

Chau D. Vo<sup>a,b</sup>, Hanna L. Shebert<sup>a,c</sup>, Shannon Zikovich<sup>a,d</sup>, Rebecca A. Dryer<sup>a,e</sup>, Tony P. Huang<sup>a,f</sup>, Lindsey J. Moran<sup>a</sup>, Juno Cho<sup>a,d</sup>, Douglas R. Wassarman<sup>a,g</sup>, Bryn E. Falahee<sup>a,h</sup>, Peter D. Young<sup>a,i</sup>, Garrick H. Gu<sup>a,j</sup>, James F. Heinl<sup>a</sup>, John W. Hammond<sup>a</sup>, Taylor N. Jackvony<sup>a,k</sup>, Thomas E. Frederick<sup>l</sup>, and Jimmy A. Blair<sup>a,\*</sup>

<sup>a</sup> Williams College, Department of Chemistry, 47 Lab Campus Drive, Williamstown, MA 01267, USA

<sup>b</sup> Present address: Johns Hopkins University School of Medicine, Baltimore, MD 21205, USA

<sup>c</sup> Present address: Department of Chemistry and Chemical Biology, Cornell University, Ithaca, NY 14853, USA

<sup>d</sup> Present address: University of Michigan Medical School, 1301 Catherine Street, Ann Arbor, MI 48109, USA

<sup>e</sup> Present address: Emory University School of Medicine, 1648 Pierce Drive NE, Atlanta, GA 30307, USA

<sup>f</sup> Present address: Harvard University, Chemical Biology Program, Cambridge, MA 02138, USA

<sup>g</sup> Present address: Department of Cellular and Molecular Pharmacology, University of California, San Francisco, San Francisco, CA 94158, USA

<sup>h</sup> Present address: Harvard Medical School, Boston, MA 02115, USA

<sup>i</sup> Present address: Columbia University Internal Medicine Residency Program, New York, NY 10032, USA

<sup>j</sup> Present address: University of Massachusetts Medical School, 55 Lake Avenue North, Worcester, MA 01655, USA

<sup>k</sup> Present address: University of Connecticut School of Medicine, 263 Farmington Avenue, Farmington, CT 06032, USA

<sup>l</sup> Department of Biochemistry & Molecular Biophysics, Washington University School of Medicine, St. Louis, MO 63110, USA

### ARTICLE INFO

#### Article history:

Received

Revised

Accepted

Available online

#### Keywords:

Antibacterial

3,4-pyrazoles

Histidine kinase

Two-component signaling

Bergat fold

### ABSTRACT

To address the growing need for new antimicrobial agents, we explored whether inhibition of bacterial signaling machinery could inhibit bacterial growth. Because bacteria rely on two-component signaling systems to respond to environmental changes, and because these systems are both highly conserved and mediated by histidine kinases, inhibiting histidine kinases may provide broad spectrum antimicrobial activity. The histidine kinase ATP binding domain is conserved with the ATPase domain of eukaryotic Hsp90 molecular chaperones. To find a chemical scaffold for compounds that target histidine kinases, we leveraged this conservation. We screened ATP competitive Hsp90 inhibitors against CckA, an essential histidine kinase in *Caulobacter crescentus* that controls cell growth, and showed that the diaryl pyrazole is a promising scaffold for histidine kinase inhibition. We synthesized a panel of derivatives and found that they inhibit the histidine kinases *C. crescentus* CckA and *Salmonella* PhoQ but not *C. crescentus* DivJ; and they inhibit bacterial growth in both Gram-negative and Gram-positive bacterial strains.

2009 Elsevier Ltd. All rights reserved.

\* Corresponding author. Tel.: +1-413-597-4417; fax: +1-413-597-4150; e-mail: [jab6@williams.edu](mailto:jab6@williams.edu).

With the worldwide rise in the frequency of drug-resistant bacterial infections, we face a critical clinical need for new therapies.<sup>10</sup> One strategy to address this need involves the development of antimicrobial agents that target novel bacterial functions, and one such class of targets is the two-component signaling (TCS) system, the signaling machinery employed by bacteria to respond to diverse environmental signals such as nutrients, quorum signals, and ions (**Figure 1A**).<sup>12, 13</sup> Bacteria rely on TCS pathways, which are mediated by histidine kinases (HKs) and absent in humans,<sup>16</sup> to respond to extracellular changes. This ability to respond and adapt is crucial for survival in the harsh environments that bacteria encounter;<sup>18</sup> hence several HKs are essential, including WalK (YycG) in *Staphylococcus aureus*<sup>20</sup> and CckA in *Caulobacter crescentus*.<sup>21</sup> This suggests that disrupting TCS pathways will provide a novel strategy for antibiotic drug discovery, because they play central roles in bacterial physiology.

Inhibition of HK function by targeting the conserved catalytic machinery of HKs is a promising strategy to disrupt TCS pathways.<sup>8, 12, 13, 17, 19</sup> Upon activation, typically from its extracellular signaling domain interacting with its target ligand, HKs bind ATP at the catalytic and ATP-binding (CA) domain and catalyze the transfer of the  $\gamma$ -phosphate of ATP to a conserved histidine residue on the HK dimerization and histidine phosphotransfer (DHp) domain (**Figure 1A**).<sup>16, 22</sup> HKs participate in a signaling cascade that transfers this phosphate group from the conserved, phosphorylated histidine on a HK to a conserved aspartic acid in a response regulator domain found on a response regulator protein (RR), the HK's cognate signaling partner (**Figure 1A**).<sup>16, 22</sup> Typical RRs are multi-domain proteins harboring both a response regulator domain and a DNA-binding domain. Activation of the RR by phosphorylation triggers the RR to bind to DNA and activate gene transcription, eliciting a genetic response to the extracellular stimulus (**Figure 1A**).<sup>16, 22</sup> ATP competitive inhibitors are one method for inhibiting these kinases, and this strategy has the potential to globally inhibit all bacterial histidine kinases, thereby affording broad-spectrum antibacterial activity.<sup>12, 13</sup> Indeed, recent drug discovery efforts in this area have demonstrated that inhibitors of multiple HKs display growth inhibition against both Gram-positive and Gram-negative bacterial strains.<sup>8, 17, 19, 23</sup>

To find a lead molecules, we asked whether inhibitors of eukaryotic Hsp90 chaperones could serve as potent lead molecules for HKs. Histidine kinases are members of the GHKL superfamily that includes four families of functionally diverse proteins: the HKs, the Hsp90 molecular chaperones, the MutL DNA-mismatch-repair enzymes, and the DNA-remodeling DNA gyrases. This superfamily is defined by the Bergerat fold, a unique ATP-binding domain crucial for ATP binding and hydrolysis and one that is not found in other protein families (**Figure 1B**).<sup>24</sup> The shared structural and sequence homology in the Bergerat fold of HKs with Hsp90 molecular chaperones suggested that Hsp90 inhibitors could also inhibit HKs (**Supplemental Figure 1**). Because cancer cells are often reliant on the activity of Hsp90 to properly fold oncogenes, Hsp90 is an important drug target in its own right for the treatment of cancer, and many inhibitors of Hsp90 have been developed, providing a selection of potential molecules for our screening efforts.<sup>25-27</sup> This strategy showed early success: Guarnieri and co-workers demonstrated that radicicol (**Figure 2**), a potent Hsp90 inhibitor, weakly bound to the *Salmonella* PhoQ HK with a  $K_d = 715 \mu\text{M}$ ,<sup>1</sup> and in a follow-up study with a small library of Hsp90 inhibitors, they found one hit, JH-II-126, that also bound weakly with a  $K_d = 391 \mu\text{M}$ .<sup>7</sup> Neither of these studies, however, demonstrated antimicrobial activity of their hits. Similarly, Boibessot *et al.* reported their rational design of HK inhibitors based on inhibitors of DNA gyrase. They found that their inhibitors, which used a thiophene scaffold, inhibited both WalK and PhoR *in vitro* and demonstrated broad-spectrum antibacterial activity.<sup>8</sup> With these efforts as inspiration, we explored whether Hsp90 inhibitors could be repurposed as antibiotics by inhibiting histidine kinases.

To this end, we purchased six commercially available Hsp90 inhibitors (**Figure 2**: NVP-AUY922,<sup>28</sup> CCT018159,<sup>29</sup> BIIB 021,<sup>30</sup> PU H71,<sup>31</sup> and CUDC-305<sup>32</sup>) and tested them against the CckA histidine kinase from *Caulobacter crescentus*, which is a nonpathogenic, Gram-negative bacterium that is a member of  $\alpha$ -proteobacteria, and it serves as a model system for bacterial cell development and two-component signal transduction.<sup>33, 34</sup> Crucially, CckA is essential in *C. crescentus*, and its activity is required for controlling cell-cycle progression as well as the transcription of more than 90 genes.<sup>21, 35-37</sup> Moreover, CckA is conserved throughout  $\alpha$ -proteobacteria,<sup>38</sup> including the plant pathogen *Agrobacterium tumefaciens*<sup>39</sup> and the zoonotic pathogen *Brucella abortus*.<sup>40</sup> To determine which Hsp90 inhibitors interacted with CckA, we formulated the inhibitors in DMSO and measured the increase in thermal stability of CckA in a ThermoFluor thermal shift assay at an inhibitor concentration of 30  $\mu\text{M}$  (**Table 1**).<sup>41-43</sup> This assay—alternatively called differential scanning fluorimetry<sup>42, 44</sup>—has recently been used in a fragment-based discovery effort against the CA domain of HKs,<sup>17</sup> in a screen for small molecules that bind the HK extracellular receptor domain of the *Staphylococcus aureus* WalK,<sup>45, 46</sup> and in a screen to identify amino acids that bind the extracellular domain of HK chemoreceptors in *Pseudomonas syringae*,<sup>47</sup> highlighting its broad utility in HK drug discovery and biochemistry. We used a construct of CckA (CckA- $\Delta 3$ ), comprised of amino acids 190–562 that includes its DHp domain, its CA domain where ATP binds, and the first of its two Per-Arnt-Sim (PAS) domains that are involved in mediating signaling.<sup>22, 48, 49</sup> We chose this construct because of its ease of expression and purification from *E. coli* and its favorable thermal denaturation properties in ThermoFluor assays. As a positive control for thermal stabilization of CckA- $\Delta 3$ , we found a thermal shift of  $3.5 \pm 0.3 \text{ }^\circ\text{C}$  using 10 mM AMPPNP, a non-hydrolyzable ATP analog. We discovered that only two Hsp90 inhibitors—NVP-AUY922 and CCT018159—shifted the melting temperature of CckA- $\Delta 3$  greater than 1.5  $^\circ\text{C}$  relative to the DMSO-only control (**Table 1**), suggesting that both these inhibitors bound tightly to CckA- $\Delta 3$ .

Hsp90 inhibitors NVP-AUY922 and CCT018159 also inhibited CckA activity *in vitro*. We measured inhibition against CckA-ATM, a construct of CckA spanning amino acids 70–691 that contains the entire cytosolic portion of CckA and includes an N-terminal His<sub>6</sub>-tag for affinity purification,<sup>21, 50</sup> using a continuous ATPase assay that couples the formation of ADP from ATP hydrolysis to NADH oxidation using a pyruvate kinase/lactate dehydrogenase (PK/LDH) coupling system.<sup>51, 52</sup> In this assay we followed the oxidation of NADH by monitoring the decrease in absorbance of NADH at 340 nm as a function of time. This assay measures the activity of any ATPase in the reaction mixture, and contaminant ATPase could lead to false positive activity. To ensure we were only measuring CckA activity, we purified a kinase-dead variant—CckA- $\Delta\text{TM}$  H322A<sup>51</sup>—using identical purification methods as the wild-type variant, and we demonstrated that its activity is negligible relative to the wild-type (**Supplemental Figure 4**). We screened all six Hsp90 inhibitors against CckA- $\Delta\text{TM}$  and found that only NVP-AUY922 and CCT018159 significantly inhibited CckA- $\Delta\text{TM}$  below 50  $\mu\text{M}$ , thereby corroborating our ThermoFluor results (**Table 1**).

NVP-AUY922 and CCT018159 share structural similarity. Both feature a central five-membered heterocycle—NVP-AUY922 includes an isoxazole, whereas CCT018159 includes a pyrazole—that connects two aromatic rings, one of which is a resorcinol ring that is essential for binding to Hsp90.<sup>29,53</sup> To explore the structure-activity relationship (SAR) of this scaffold, we synthesized a small panel of CCT018159 analogs. We chose to focus on analogs of CCT018159 because these inhibitors could be readily synthesized in three steps and because our thermal shift data suggested CCT018159 interacted with CckA more tightly than NVP-AUY922. Furthermore, these pyrazole derivatives have been reported during the development of CCT018159 as an Hsp90 inhibitor.<sup>54-56</sup> This library was designed to allow us to explore the steric and electronic effects of the 4-position of the resorcinol ring, because substitutions at this position were shown to be important for activity against Hsp90,<sup>29,53</sup> and we asked whether similar effects played a role in HK inhibition. Likewise, we designed inhibitors with and without a 5-methyl pyrazole core to explore steric effects of the pyrazole ring. Finally, we explored three different aromatic rings off the pyrazole 4-position to ask whether increased polar character and size affects potency and solubility.

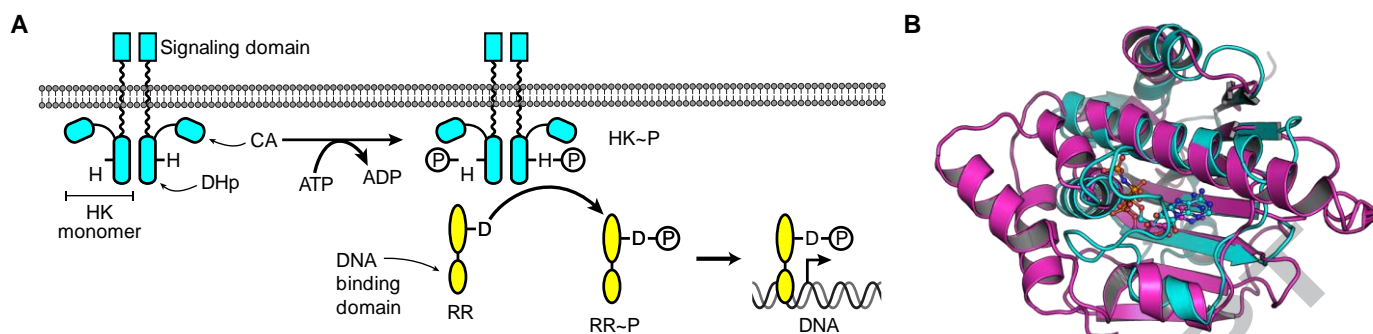


**Figure 1.** (A) A typical TCS pathway. The conserved histidine residue (H) is illustrated on the HK (cyan) in the DHp domain. Likewise, the conserved aspartic acid residue (D) on the RR (yellow) is shown. (B) A structure-based alignment<sup>3,4</sup> of the CA domain of the CckA HK (PDB 5IDM<sup>5</sup>, cyan) and the ATPase domain of yeast Hsp90 (PDB 1AMW<sup>11</sup>, magenta). Co-crystallized nucleotides (AMPPNP, CckA; ADP, Hsp90) are shown as ball-and-sticks. Core structural features surrounding the nucleotides are highly conserved. These domains share 12% sequence identity. RMSD of aligned C<sub>α</sub> atoms is 1.92 Å (87 residues).<sup>18</sup>

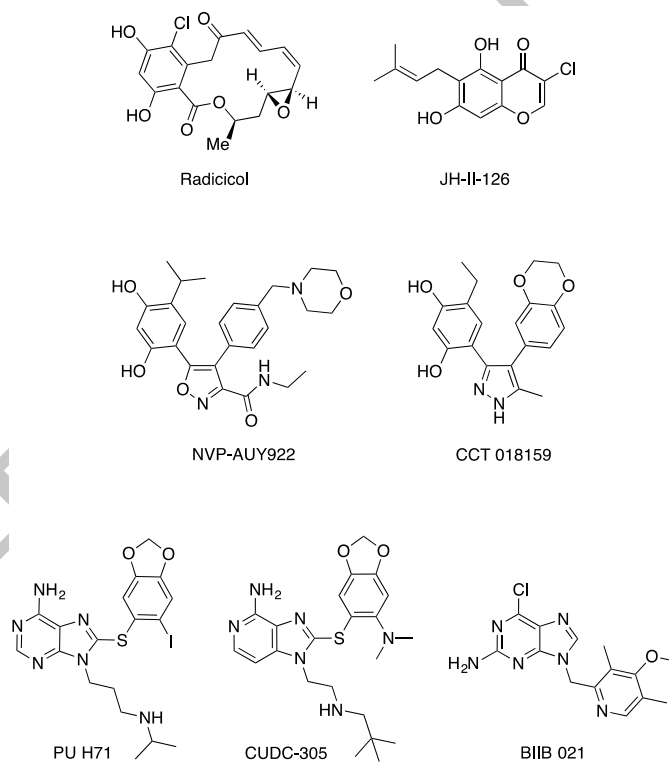
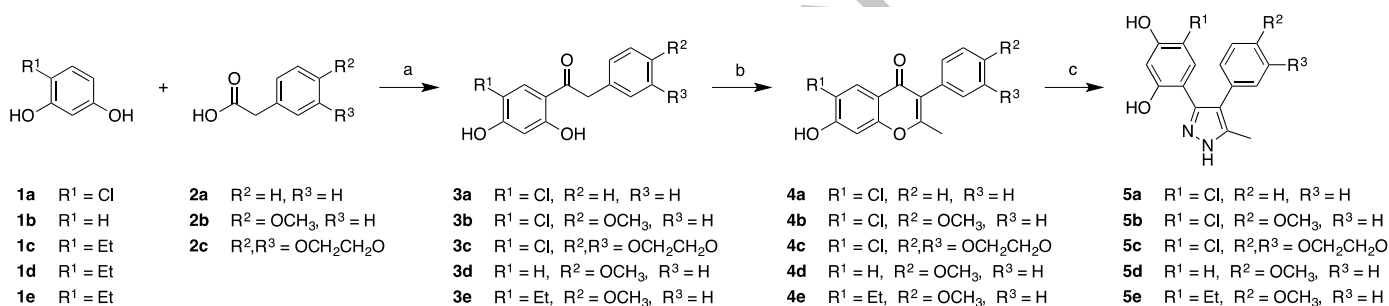


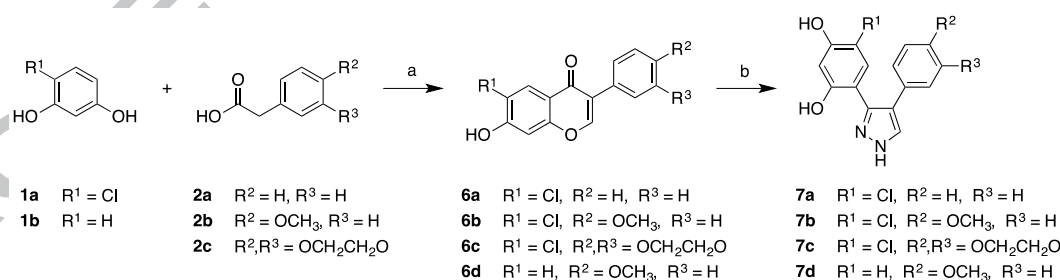
**Figure 2.** Hsp90 inhibitors. Guarnieri *et al.* demonstrated that radicolol<sup>1,2</sup> and JH-II-126<sup>7</sup> bind the PhoQ HK.

We synthesized a small library of diaryl pyrazoles following synthetic schemes described by Cheung<sup>29</sup> and Drysdale.<sup>53</sup> Inhibitors were prepared in two or three steps from commercially available resorcinols and phenylacetic acids. **Scheme 1** shows the synthetic route to 3,4-diarylpyrazoles **5a–e** with a methyl group at the 5-position of the pyrazole ring. This three-step synthesis begins with forming dihydroxyphenyl ketones **3a–e** via Friedel-Crafts acylation of the respective resorcinols and substituted phenylacetic acids using boron trifluoride diethyletherate ( $\text{BF}_3 \cdot \text{OEt}_2$ ) as a Lewis acid catalyst. These products were then refluxed with acetic anhydride in the presence of potassium carbonate to form alkylated isoflavones **4a–e**, which are then converted to the final 3,4-diaryl pyrazoles **5a–e** by the heating the isoflavones with hydrazine hydrate. To synthesize inhibitors **7a–d**, which lacked a 5-methyl group on the pyrazole ring, we used a one-pot method<sup>57</sup> to synthesize isoflavones **6a–d**, followed by pyrazole ring formation. In **Scheme 2** isoflavones **6a–d** are first formed by Friedel-Crafts acylation between resorcinols and substituted phenylacetic acids using  $\text{BF}_3 \cdot \text{OEt}_2$ , followed by addition of freshly prepared *N,N'*-dimethyl(chloromethylene) ammonium chloride, the Vilsmeier reagent, which we generated in a separate reaction between  $\text{PCl}_5$  and DMF. The second step of this scheme involves the formation of unalkylated pyrazoles **7a–d** by refluxing **6a–d** with hydrazine hydrate in a manner similar to the final step of **Scheme 1**.

We then tested these inhibitors against CckA using both thermal shift binding assays and ATP hydrolysis assays (**Table 1**). Our results show that inhibitors **5a**, **5b**, and **5c** were the most potent out of this series. We found that the 4-chlororesorcinol group was important for potency (compare **5b** to **5d** and **5e**, **Table 1**), while the substitution pattern of the aromatic ring at the 4-position had less of an impact on binding. The methyl substitution at the 5-position of the pyrazole ring also increased potency (compare **5b** to **7b**, **Table 1**). The  $\text{IC}_{50}$  values for inhibition of yeast Hsp90 ATPase activity in the presence of 370  $\mu\text{M}$ <sup>54,56</sup> or 400  $\mu\text{M}$ <sup>29</sup> ATP have been reported by others for six compounds in this study (radicol, 0.26  $\mu\text{M}$ ;<sup>56</sup> CCT018159, 7.1  $\mu\text{M}$ ;<sup>29</sup> **5a**, 1.65  $\mu\text{M}$ ;<sup>29</sup> **5b**, 1.7  $\mu\text{M}$ ;<sup>54</sup> **5c**, 0.65  $\mu\text{M}$ ;<sup>54</sup> and **5d**, 36.9  $\mu\text{M}$ <sup>54</sup>). Comparing our biochemical results for inhibition of CckA (**Table 1**) to those against Hsp90, we see that this series of diaryl pyrazoles shows greater potency for yeast Hsp90 than for CckA by approximately a factor of ten. Radicol, however, is very potent against Hsp90 but very weakly potent against CckA, highlighting that despite the similarity of these molecular targets, there is selectivity in inhibitor binding between the two proteins.



**Scheme 1.** (a)  $\text{BF}_3 \cdot \text{OEt}_2$ , 80 °C, overnight; (b) acetic anhydride,  $\text{K}_2\text{CO}_3$ , DMF, 160 °C, 4 h; (c) hydrazine hydrate, ethanol, 60 °C, 1 h.



**Scheme 2.** (a) one pot: (i)  $\text{BF}_3 \cdot \text{OEt}_2$ , 80 °C, overnight, (ii)  $\text{PCl}_5$  and DMF reacted independently, then added, rt, 1h; (b) hydrazine hydrate, ethanol, 60 °C, 1 h

**Table 1.** ThermoFluor and inhibition data against the CckA HK.

Compound	CckA- $\Delta 3$ thermal shift <sup>a</sup> $\Delta T_m \pm$ SD ( $^{\circ}$ C)	CckA- $\Delta$ TM inhibition <sup>c</sup> ATPase IC <sub>50</sub> / $\mu$ M
Radicicol	0.9 $\pm$ 0.4	184 (160–212)
NVP-AUY922	1.8 $\pm$ 0.2	7.3 (6.2–8.6)
CCT018159	4.0 $\pm$ 0.2	28.0 (20.6–38.1)
BIIB 021	0.7 $\pm$ 0.5	87% activity at 250 $\mu$ M <sup>d</sup>
PU H71	0.5 $\pm$ 0.4	61% activity at 250 $\mu$ M <sup>d</sup>
CUDC-305	0.4 $\pm$ 0.5	79% activity at 250 $\mu$ M <sup>d</sup>
AMPPNP	3.5 $\pm$ 0.3 <sup>b</sup>	n.t.
<b>5a</b>	4.5 $\pm$ 0.2	17.5 (16.1–19.0)
<b>5b</b>	5.0 $\pm$ 0.5	12.3 (10.8–14.0)
<b>5c</b>	5.3 $\pm$ 1.0	11.2 (9.7–13.0)
<b>5d</b>	2.5 $\pm$ 0.1	46.0 (39.4–53.7)
<b>5e</b>	4.1 $\pm$ 0.5	18.6 (16.1–21.4)
<b>7a</b>	3.5 $\pm$ 0.6	33.6 (27.8–40.7)
<b>7b</b>	4.2 $\pm$ 0.5	32.7 (28.5–37.6)
<b>7c</b>	3.3 $\pm$ 0.3	32.3 (29.5–35.4)
<b>7d</b>	3.5 $\pm$ 1.2	56.9 (48.4–66.8)

<sup>a</sup> Mean thermal shift of  $T_m$ , the midpoint of the thermal denaturation curve, relative to DMSO control;  $n = 4$ – $6$ ; conditions included 1.6  $\mu$ M kinase and 30  $\mu$ M of each compound; thermal melt curves are shown in **Supplemental Figures 2–3**; SD = standard deviation.

<sup>b</sup> Mean thermal shift of  $T_m$ , the midpoint of the thermal denaturation curve, relative to ultrapure water control;  $n = 4$ ; conditions included 1.6  $\mu$ M kinase and 10 mM AMPPNP; thermal melt curves are shown in **Supplemental Figure 2**; SD = standard deviation.

<sup>c</sup> IC<sub>50</sub> (95% confidence interval);  $n = 2$ ; conditions included 5  $\mu$ M kinase and 100  $\mu$ M ATP; n.t. = not tested.

<sup>d</sup> Highest concentration of compound test was 250  $\mu$ M; percent activity represents the residual ATPase activity measured at this concentration.

Inhibition of multiple HKs may provide broad-spectrum antibacterial activity,<sup>12, 13</sup> and recent drug discovery efforts<sup>8, 17, 19</sup> against HKs have focused on the development of pan-HK inhibitors. To test whether the compounds described here inhibit HKs other than CckA, we measured the inhibition of two additional HKs, *Salmonella typhimurium* PhoQ, which is involved in Mg<sup>2+</sup> sensing and is required for virulence,<sup>58, 59</sup> and *Caulobacter crescentus* DivJ, which regulates cellular differentiation.<sup>60, 61</sup> We chose PhoQ and DivJ as targets because of their diversity in the ATP-binding site: in the N-box of the HK catalytic core<sup>24, 62</sup> sits a residue conserved as a Phe, Tyr, His, or Ala, and the aromatic amino acids are unique to HKs among GHKL family members.<sup>6, 12, 63, 64</sup> Residues at this position sit above ATP, and aromatic sidechains—for example, Tyr393 in *E. coli* PhoQ (**Supplemental Figures 1 and 5**)<sup>6</sup>—make  $\pi$ - $\pi$  stacking interactions with the adenine ring. Wilke and Carlson hypothesized that these residues could be exploited to endow selectivity toward HKs,<sup>12</sup> and because PhoQ has Tyr, DivJ has Phe, and CckA has Ala at this position, we felt this suite of HKs could help define the role this residue position played in inhibitor binding. We note that at this same position Hsp90 contains an Ala residue (**Supplemental Figure 1**), as does CckA. We expressed and purified *C. crescentus* DivJ and *Salmonella typhimurium* PhoQ. Each construct included the DHP-CA domains necessary for catalysis, with the DivJ construct<sup>49, 65</sup> spanning residues 188–585 and including an N-terminal His<sub>6</sub>-tag, and the PhoQ construct spanning residues 257–487<sup>1</sup> and including an N-terminal His<sub>6</sub>-SUMO tag for affinity purification and protein solubility.<sup>66</sup> We used a radioactive phosphotransfer assay in a dot blot format<sup>49</sup> that measures the transfer of the  $\gamma$ -<sup>32</sup>P-phosphate from [ $\gamma$ -<sup>32</sup>P]-ATP to the HK. This assay has been used to quantify the *in vitro* activity of CckA and DivJ both in solution and on liposomes.<sup>49</sup> Initially, we screened all Hsp90 inhibitors and our synthesized diaryl pyrazoles at 500  $\mu$ M against DivJ and PhoQ, quantifying the percent autophosphorylation relative to a DMSO-only control. Inhibitors showed selectivity between these HKs: treating with diaryl pyrazoles or NVP-AUY922 lowered PhoQ phosphotransfer activity to 9–87% of an untreated control but failed to lower DivJ phosphotransfer activity, with only CCT018159 showing DivJ activity below 85% (70% activity, **Table 2**). Hsp90 inhibitors BIIB 021, PU H71, and CUDC-305 showed little-to-no inhibition of either PhoQ or DivJ, which is consistent with our results with CckA (**Table 1**). We then selected a subset of these inhibitors—NVP-AUY922, CCT018159, **5b**, **5c**, and **7c**—to characterize their dose-response activity against all three HKs in a phosphotransfer assay. Inhibition assays confirmed the selectivity these inhibitors show: they inhibit CckA- $\Delta$ TM (IC<sub>50</sub> = 14–44  $\mu$ M) more potently than PhoQ (IC<sub>50</sub> = 238–270  $\mu$ M), and they show no measurable inhibition at 800  $\mu$ M against DivJ. CCT018159 inhibited all activity of DivJ at 800  $\mu$ M, which represented a very steep dose-response between 400  $\mu$ M and 800  $\mu$ M, suggesting a non-specific mechanism<sup>67</sup> of CCT018159 against DivJ, which we attribute to aggregation of DivJ at high CCT018159 concentrations (see below). These data suggest that the topology of the HK active site shows diversity that may be difficult

to globally exploit, and they highlight that diaryl pyrazoles may not effectively exploit the conserved aromatic rings as a selectivity filter between HKs and Hsp90.

**Table 2.** Inhibitory data against multiple histidine kinases.

Compound	PhoQ autophosphorylation <sup>a</sup> Mean % activity ± SD	DivJ autophosphorylation <sup>a</sup> Mean % activity ± SD	PhoQ inhibition <sup>b</sup> IC <sub>50</sub> / μM	DivJ inhibition <sup>b</sup> IC <sub>50</sub> / μM	CckA-ΔTM inhibition <sup>b</sup> IC <sub>50</sub> / μM
Radicol	86 ± 10	123 ± 13	n.t.	n.t.	n.t.
NVP-AUY922	73 ± 3	109 ± 16	56% activity at 800 μM <sup>c</sup>	No inhibition	28 (21–37)
CCT018159	9 ± 7	70 ± 8	261 (200–339)	No inhibition <sup>d</sup>	30 (21–45)
BIIB 021	87 ± 8	128 ± 2	n.t.	n.t.	n.t.
PU H71	103 ± 12	122 ± 14	n.t.	n.t.	n.t.
CUDC-305	110 ± 23	96 ± 17	n.t.	n.t.	n.t.
<b>5a</b>	45 ± 3	115 ± 5	n.t.	n.t.	n.t.
<b>5b</b>	66 ± 8	118 ± 20	238 (195–289)	No inhibition	14 (10–20)
<b>5c</b>	35 ± 2	113 ± 20	270 (220–332)	No inhibition	28 (18–42)
<b>5d</b>	76 ± 2	117 ± 9	n.t.	n.t.	n.t.
<b>5e</b>	36 ± 3	118 ± 6	n.t.	n.t.	n.t.
<b>7a</b>	63 ± 10	92 ± 12	n.t.	n.t.	n.t.
<b>7b</b>	62 ± 4	112 ± 6	n.t.	n.t.	n.t.
<b>7c</b>	63 ± 4	117 ± 14	48% activity at 800 μM <sup>c</sup>	No inhibition	44 (30–65)
<b>7d</b>	87 ± 10	85 ± 10	n.t.	n.t.	n.t.

<sup>a</sup> Relative phosphotransfer as a percentage of DMSO-only control, which gives 100% activity;  $n = 3$ ; conditions included 4.5 μM kinase, 3 μM ATP, and 500 μM of each compound; SD = standard deviation.

<sup>b</sup> IC<sub>50</sub> (95% confidence interval);  $n = 2$ ; conditions included 4.5 μM kinase and 3 μM ATP; n.t. = not tested.

<sup>c</sup> Highest concentration of compound test was 800 μM; percent activity represents the residual ATPase activity measured at this concentration.

<sup>d</sup> No inhibition observed at 400 μM CCT018159; at 800 μM, complete inhibition is observed, which we attribute to non-specific aggregation.

First generation HK inhibitors were found to demonstrate non-specific inhibition through protein aggregation,<sup>63, 68</sup> and recent HK inhibitor discovery efforts have shown the utility of gel-based aggregation studies to identify aggregators.<sup>17, 19, 63</sup> To assess whether the inhibitors caused non-specific protein aggregation, we screened inhibitors against all four proteins to determine whether inhibitors caused HK aggregation under the conditions we measured our biochemical assays. After incubation of compounds with each HK, we separated each reaction by native polyacrylamide gel electrophoresis (native-PAGE) and visualized protein migration with colloidal coomassie staining. We included negative controls of DMSO and ultrapure water, and we included Congo Red, a known protein aggregator that displays nonspecific enzyme inhibition through aggregation,<sup>69</sup> as a positive control. Inhibitors reported in this study did not aggregate CckA at up to 333 μM (**Figure 3**), and a subset of these inhibitors screened against DivJ and PhoQ demonstrated no aggregation at 400 μM, and only CCT018159 caused aggregation at 800 μM with DivJ (**Figure 3**). These results are consistent with our phosphotransfer assay results for CCT018159 with DivJ, where we observed no inhibition at 400 μM and complete inhibition at 800 μM (**Table 2**), and we attribute this behavior to aggregation of DivJ by CCT018159. We note that CCT018159 does not aggregate PhoQ at 800 μM, suggesting that native-PAGE aggregation studies have some target-based bias.

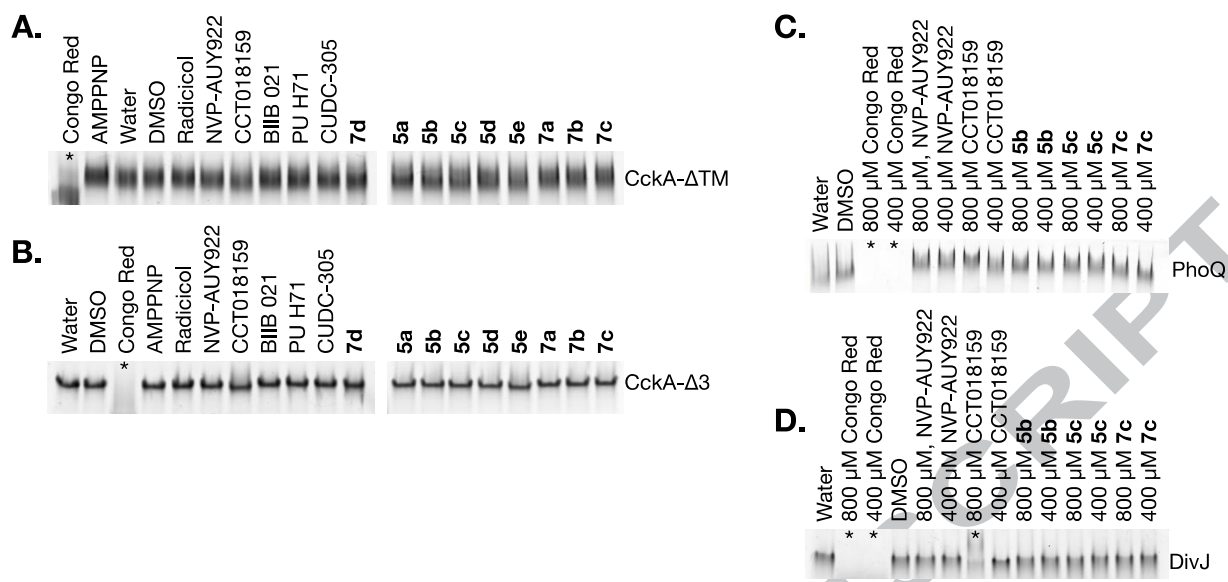


**Figure 3.** Gel-based aggression studies using Native-PAGE. Congo Red is a positive control for protein aggregation. (A) Conditions: 4.5  $\mu\text{M}$  CckA- $\Delta\text{TM}$ , 333  $\mu\text{M}$  compound, 5% (v/v) DMSO. (B) Conditions: 4.5  $\mu\text{M}$  CckA- $\Delta\text{3}$ , 333  $\mu\text{M}$  compound, 5% (v/v) DMSO. (C) Conditions: 4.7  $\mu\text{M}$  PhoQ, 400 or 800  $\mu\text{M}$  compound, 10% (v/v) DMSO, 10% (v/v) glycerol. (D) Conditions: 4.5  $\mu\text{M}$  DivJ, 400 or 800  $\mu\text{M}$  compound, 10% (v/v) DMSO, 10% (v/v) glycerol. We denote protein shifts indicative of protein aggregation (\*).

In addition, first generation HK inhibitors also caused membrane damage and hemolysis,<sup>70</sup> demonstrating a general cytotoxicity that suggested those early chemical leads were poor starting points for antibiotic development. In an effort to define whether the inhibitors described in this study demonstrate adverse effects on cell membranes, we screened inhibitors in a hemolysis assay for cell lysis. We incubated 0.5 mM of each compound with citrated sheep red blood cells, and we determined the percentage of cell lysis by measuring the absorbance of hemoglobin at 540 nm in cleared cell lysates in the presence of each compound compared to a positive control treated with 1% (v/v) Triton X-100, which causes complete cell lysis and release of hemoglobin (**Table 3**). We found that the inhibitors reported here show minimal hemolysis of sheep red blood cells with only CCT018159 (14%) and **5e** (15%) showing hemolysis greater than 3% among diaryl pyrazoles. Inhibitors CCT018159 and **5e** are the only diaryl pyrazoles reported here that contain an ethyl substituent at the 4-position of the resorcinol ring, suggesting that placing a nonpolar substituent at this position leads to undesirable effects on membrane integrity.

To determine the mechanism of inhibition of diaryl pyrazoles against CckA, we measured the enzyme activity while varying both the concentration of substrate ATP and inhibitor **5b**. Given the structural similarity between HKs and Hsp90, we hypothesized that analogs of CCT018159 would bind the HK ATP-binding site and therefore be competitive inhibitors of HKs because crystallographic studies of Hsp90 with CCT018159 (PDB 2BRC)<sup>29</sup> or NVP-AUY922 (PDB 2VCI)<sup>28</sup> show that these inhibitors bind to the ATP-binding site of Hsp90. Using our ATPase coupled enzyme assay with CckA- $\Delta\text{TM}$ , we measured the initial velocity at each inhibitor concentration and substrate concentration (**Figure 4**). The data were fit to enzyme inhibition models with shared  $V_{\text{max}}$ ,  $K_{\text{m}}$ , and  $K_{\text{i}}$  parameters.<sup>71</sup> The data fit best to a competitive model of inhibition, which is consistent with our hypothesis that these inhibitors bind to the ATP-binding site of CckA. Given the close structural similarity among the diaryl pyrazoles, we predict that other diaryl pyrazoles inhibit HKs competitively with ATP.

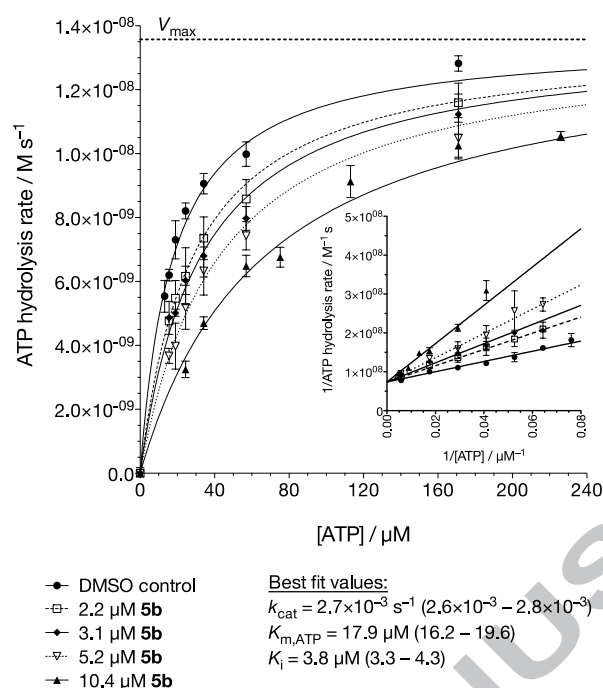


**Figure 4.** Inhibitor **5b** inhibits the CckA HK competitively with ATP. Inset, Lineweaver-Burk plot. Initial rates were measured in triplicate, and the mean and standard deviation are shown. The best fit values (95% confidence interval) for a competitive inhibition model are shown. 5 μM CckA-ΔTM was used.

Because **5b** inhibited CckA competitively, we asked which molecular interactions mediated binding to the ATP-binding site. To predict these interactions, we performed molecular docking studies of **5a–e** and **7a–d** with both CckA and PhoQ. For these calculations, we chose crystal structures of the CA domains of *C. crescentus* CckA (PDB 5IDM<sup>5</sup>) and *E. coli* PhoQ (PDB 1ID0<sup>6</sup>) that each contained the ATP-analog AMPPNP and a fully defined ATP lid, a flexible loop involved in nucleotide binding.<sup>24, 64</sup> We prepared the targets using the OEDocking toolkit<sup>72</sup> by retaining a fragment of AMPPNP (AMPPNP trimmed back to 9-methyladenine) and two conserved water molecules that make direct polar interactions with the adenine ring of AMPPNP. Using HYBRID,<sup>73</sup> which uses a ligand-guided approach to docking, we docked the diaryl pyrazole inhibitors, NVP-AUY922, and AMPPNP to each target with constraints for polar interactions with both retained water molecules and a conserved Asp (Asp479 in CckA; Asp415 in *E. coli* PhoQ) in the D/G1-box that hydrogen bonds to the N6 exocyclic amine of ATP. The top-scoring predicted binding modes of **5b** are shown in **Figure 5A–B**, and **Supplementary Figures 6–7** show the remaining top-scoring docking results. The docking poses of AMPPNP compared closely (RMSD <0.8 Å for 11 atoms) with identical atoms in the guide ligand, suggesting a successful re-docking of the ligand and validation of this method (**Supplementary Figures 6–7**). The docking modes of **5b** in both CckA and PhoQ were nearly identical (**Figure 5A–B**), suggesting the key binding interactions between CckA and PhoQ are similar. Importantly, the predicted binding pose suggests that **5b** makes direct hydrogen-bonding interactions with the D/G1-box conserved Asp in the active site through both hydroxyl groups of the resorcinol ring. This interaction is an important recognition element for the GHKL super family<sup>24</sup>: it is a key element in the binding of ATP-competitive inhibitors against Hsp90 (for example, **Figure 5C**<sup>9</sup>), and this same interaction is seen in the PhoQ-radical structure (PDB 3CGY), the sole crystal structure of an HK bound with a ligand other than an ATP analog at the ATP-binding site.<sup>1</sup> These poses help explain, in part, the SAR we observe, where the 4-chlororesorcinol derivatives **5a–c** and **7a–c** are more potent than the ethylresorcinol **5e** and resorcinol (**5d**, **7d**) derivatives. Substituents at the 4-position of the resorcinol ring are predicted to occupy a pocket largely composed of hydrophobic residues with a single, conserved Asn “lid” of the N-box (Leu446-Met472-Val386-Asn389 in PhoQ; Leu510-Phe536-Val431-Asn434 in CckA). The predicted inhibitor binding modes suggest that larger aliphatic substituents such as 4-ethyl in CCT018159 and **5e** may not provide an optimal fit in to this pocket, while inhibitors lacking any substitution at 4-resorcinol position do not complement this pocket. The 4-chlororesorcinol derivatives may inhibit best because they include a substituent at the 4-resorcinol position that fills this pocket with enough polar character to limit unfavorable hydrophobic interactions with the conserved Asn “lid”. The most common pose for inhibitors **5a–e**, which contain a 5-methyl group on the pyrazole ring, positions the 5-methyl group pointed out toward solvent in PhoQ and within 2.4 Å of Thr499 and 3.6 Å of Phe497 in CckA. We are unable to explain the increased potency of this series relative to **7a–d**, but we speculate that perhaps it makes favorable hydrophobic contacts with the flexible ATP-lid. Taken together, these data suggest the active sites of two different HKs accommodate diaryl pyrazoles via similar chemical interactions.

Moreover, the predicted poses of the diaryl pyrazole inhibitors illustrate a potential strategy for developing HK-selective inhibitors from this series. Our PhoQ docking model for all the inhibitors described here show an important  $\pi$ - $\pi$  stacking interaction with Tyr393 of the conserved N-box, which is a hydrophobic interaction observed between the adenine ring of AMPPNP and PhoQ (PDB 1ID0<sup>6</sup>) (**Figure 5B**, **Supplementary Figure 7**). This same  $\pi$ - $\pi$  stacking interaction has been reported for similar docking studies with

compounds that share little structural similarity with the diaryl pyrazole scaffold, suggesting that this interaction is key for maintaining productive ligand-protein interactions at the ATP-binding site of HKs.<sup>8, 17, 63</sup> HKs conserve Ala, Tyr, Phe, and His at this site of the N-box (**Supplementary Figures 1 and 5**),<sup>6, 12, 63</sup> and because the aromatic residues Tyr, Phe, and His are conserved only in HKs among the GHKL family members, Wilke and Carlson proposed exploiting this interaction as a selectivity filter between HKs and gyrase B, MutL, and Hsp90.<sup>12</sup> Our docking results support this hypothesis. A structure-based sequence alignment of the CA domain of HKs with the Hsp90 ATPase domain shows that Hsp90 bears an Ala residue (Ala41, yeast; Ala55, human) at the end of the N-box where PhoQ bears Tyr393 (**Supplementary Figure 1**). This smaller residue opens additional space within the N-box helix in Hsp90 compared to PhoQ, and consequently, in crystals structures of diaryl pyrazoles bound to Hsp90—for example Hsp90 bound with VER-49009 (PDB 3OWB<sup>9</sup>), a close structural analog of **5b** (**Figure 5C**)—the pyrazole ring pivots toward the N-box helix relative to the docking mode calculated for PhoQ and CckA (**Figure 5A–B**). A structural alignment of the PhoQ-**5b** docking result with Hsp90-VER-49009 illustrates that the PhoQ HK is likely unable to accommodate the Hsp90-like binding mode because of direct steric interactions with Tyr393 (**Figure 5D**). Therefore, we hypothesize that molecules that maintain the favorable  $\pi$ - $\pi$  interactions with the N-box aromatic residues and the hydrogen-bonding interactions with the D/G1-box Asp and ordered waters in the active site but are unable to pivot may provide selectivity for HKs over Hsp90 inhibitors. What is striking is that CckA harbors Ala at this same position (Ala438), yet the predicted binding mode adopts the PhoQ-like trajectory of the diaryl pyrazole rather than the Hsp90-like mode. It is tempting to suggest that N-box aromatic residues are not strictly necessary to differentiate the HK active site from an Hsp90 active site, and we believe structural evidence of a diaryl pyrazole bound to CckA bound would help resolve this outstanding question. We note that one possible strategy to select for HK inhibition over Hsp90 inhibition could include exploiting the F-box,<sup>12, 13</sup> a sequence motif that appears N-terminal to the ATP-lid, that contains at least one Phe residue, and that is conserved in HKs but not other GHKL members.<sup>24</sup> Our docking results (**Figure 5A–B**) place this motif approximately 10.5 Å away from the C4-position of the pyrazole ring among our diaryl pyrazoles, suggesting that derivatives at the pyrazole C4-position may be able to exploit this motif. Future work will focus on the design of derivative molecules that bind the HK fold but have lost interaction with Hsp90 and other GHKL family members.

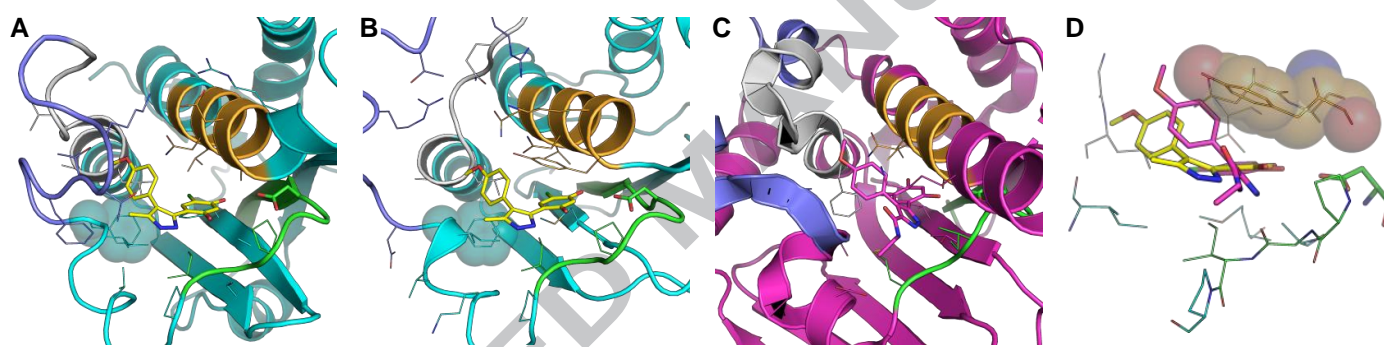


**Figure 5.** (A) Predicted binding mode of **5b** with the CckA CA domain. The top-scoring pose of **5b** with CckA (PDB 5IDM<sup>5</sup>) is shown. (B) Predicted binding mode of **5b** with the PhoQ CA domain. The top-scoring pose of **5b** with PhoQ (PDB 1ID0<sup>6</sup>) is shown. For (A) and (B) the HK is cyan with key conserved HK elements highlighted (N-box, orange; D/G1-box, green; ATP lid, slate blue; G2-box, white/grey), amino acid sidechains within 5 Å of **5b** are shown as lines, **5b** is yellow sticks, the conserved Asp that hydrogen bonds to the exocyclic ATP nitrogen is green sticks, and the conserved first Phe of the F-box is shown as transparent, cyan spheres. (C) Co-crystal structure (PDB 3OWB<sup>9</sup>) of human Hsp90 with VER-49009, a close structural analog of **5b**. Hsp90 is magenta, and motifs conserved with HKs are highlighted as above. (D) Docked binding mode of **5b** with PhoQ overlaid with VER-49009 from Hsp90. PhoQ Tyr 393 is shown as transparent, orange spheres.

We next aimed to demonstrate that the inhibitory activity of CCT018159 analogs against HKs *in vitro* translated to an *in vivo* model. We used the broth-dilution method to determine the minimum inhibitory concentration (MIC) of these compounds (**Table 3**).<sup>74</sup> We tested inhibitor susceptibility against model Gram-positive (*B. subtilis* YB886<sup>75</sup>) and Gram-negative strains (*E. coli* DC2<sup>76, 77</sup> and *C. crescentus* NA1000<sup>78</sup>). In terms of conservation of the HKs we assayed for biochemical inhibition among these three bacterial strains, CckA and DivJ are only found in *C. crescentus*, and PhoQ is only found in *E. coli*. Because we did not know whether these inhibitors would cross into the bacterial cytoplasm, where the ATP-binding domains of HKs reside, we used *E. coli* DC2, which is a strain hypersensitive to antibiotics due to increased cell permeability.<sup>76, 77</sup> Inhibitors were most potent against *E. coli* DC2, which we expected based on the increased susceptibility to antibiotics this strain exhibits, and were least potent against *C. crescentus*, a Gram-negative strain (**Table 3**). Inhibitor **5b**, which effectively inhibited both CckA and PhoQ *in vitro*, was also effective at inhibiting bacterial growth of each strain. Generally, the chlororesorcinol derivatives **5a–c** and **7a–c** were more potent than the ethylresorcinol **5e** and resorcinol (**5d**, **7d**) derivatives. Comparing inhibitor **5b** to our lead molecule CCT018159, we see that while **5b** inhibits and stabilizes CckA better than CCT018159 (**Table 1**), CCT018159 inhibits antimicrobial growth at lower concentrations for both *C. crescentus* and *B. subtilis*. Of the Hsp90 inhibitors we originally screened (radicol, NVP-AUY922, CCT018159, BIIB 021, PU H71, and CUDC-305), only the diaryl pyrazole CCT018159 inhibited *C. crescentus* and *B. subtilis* growth at or below 300  $\mu$ M, and radicol, which Guarnieri demonstrated bound weakly to *Salmonella* PhoQ HK<sup>1, 7</sup> and which we found only weakly inhibited CckA, did not inhibit bacterial growth. We note that CCT018159 demonstrated mild hemolysis effects at 0.5 mM and aggregated DivJ at 0.8 mM, suggesting that its mechanism of action may be due in part to membrane disruption. Future experiments will explore the mechanisms of antimicrobial action, including whether these inhibitors cause membrane disruption against bacteria, and whether they display bacteriostatic or bactericidal effects.

The diaryl pyrazoles reported here demonstrate similar potency with recently described HK inhibitors (**Figure 6**). Recent drug discovery efforts have utilized virtual screening (Liu,<sup>15</sup> Lv,<sup>14</sup> Velikova<sup>17</sup>), fragment-based screening (Velikova<sup>17</sup>), structure-based drug design (Boibessot<sup>8</sup>), and high-throughput screening methods (Wilke<sup>19</sup>), and each method has yielded promising lead scaffolds for antibiotics targeting HKs. Our method, which focuses on repurposing drug-like molecules that inhibit a conserved superfamily member, demonstrates that lead molecules of comparable efficacy may be developed using rational design approaches. In biochemical assays for either ATPase activity (this study, Liu,<sup>15</sup> and Lv<sup>14</sup>) or phosphotransfer assays (this study, Boibessot,<sup>8</sup> Velikova,<sup>17</sup> and Wilke<sup>19</sup>), the IC<sub>50</sub> values span roughly two orders of magnitude. For example Wilke 11<sup>19</sup> has an IC<sub>50</sub> of 1.21  $\mu\text{M}$  against *T. maritima* HK853, and **5d** has an IC<sub>50</sub> of 238  $\mu\text{M}$  against *S. typhimurium* PhoQ (**Figure 6**). Compared to the best HK inhibitors described to date (Lv H2-81<sup>14</sup> and Liu H5-33,<sup>15</sup> which have ATPase IC<sub>50</sub> values of 24  $\mu\text{M}$  against *Staphylococcus epidermidis* WalK and MIC values against Gram-positive *S. epidermidis* of  $<2 \mu\text{g mL}^{-1}$ ), our inhibitors show similar biochemical activity but are less active at inhibiting bacterial growth. We have not tested our inhibitors against WalK or *S. epidermidis*, so these differences may be target specific. Furthermore, only Wilke and co-workers, who measured drug binding by displacement of a fluorescently labeled ATP-analog,<sup>19</sup> and this study have demonstrated direct competition of inhibitors with ATP; thus it remains possible that other reported HK inhibitors work by another mechanism that leads them to be more potent *in vivo*. Because the biochemical assays use different ATP concentrations, and HKs have a wide range of  $K_m$  values for ATP ( $\sim 2.4\text{--}300 \mu\text{M}$ , see Trajtenberg<sup>79</sup>), we note that direct comparisons between each study should be made with caution. That said, two general trends appear. First, each inhibitor typically shows a range of potencies for HKs (**Figure 6**), suggesting one pharmacophore may not be able to potently inhibit HKs universally. And second, the MIC values for Gram-negative bacteria typically are higher than Gram-positive strains. For example, Boibessot 6d<sup>8</sup> has an MIC that is 4.5 $\times$  higher for *E. coli* than *B. subtilis*, while Velikova and co-workers<sup>17</sup> found that S1.13 did not affect *E. coli* growth at 500  $\mu\text{g mL}^{-1}$  despite having an MIC of 8  $\mu\text{g mL}^{-1}$  against *S. aureus* (**Figure 6**). In this study, we found that **5b** has a comparable MIC between *C. crescentus* and *B. subtilis*. These strain-related differences may be attributed in part to membrane permeability: like Wilke and co-workers,<sup>19</sup> we used *E. coli* DC2, a strain with a compromised cell membrane,<sup>76, 77</sup> and found higher potency of our diaryl pyrazoles with this strain compared to *C. crescentus*, which is not hypersensitive to antibiotics. Recent work by Velikova and co-workers involving encapsulation of HK inhibitors in  $\epsilon$ -poly-L-lysine capped nanoparticles supports this hypothesis.<sup>23</sup> For example, they demonstrated that capped nanoparticles harboring inhibitor Velikova S1.13 had an MIC against *E. coli* CFT 073 of 25  $\mu\text{g mL}^{-1}$ , which is more than tenfold lower than Velikova S1.13, and these effects were attributed to the ability of  $\epsilon$ -poly-L-lysine capped nanoparticles to associate with the bacterial outer membrane, followed by release of the HK inhibitor cargo inside the cell, thereby bypassing the protective outer membrane Gram-negative bacteria contain.<sup>23</sup> In addition, these effects may be explained by the fact that *E. coli* does not contain essential HKs,<sup>80, 81</sup> whereas *C. crescentus* has four (CckA, CenK, DivL, PetR),<sup>35, 37</sup> and *B. subtilis* has one (YycG, which is also known as WalK or VicK).<sup>82, 83</sup> Future experiments will focus on distinguishing between these two potential modes of action.

Finally, we recognize that the diaryl pyrazoles, like many other HK inhibitors (**Figure 6**), inhibit growth only at relatively high concentrations ( $\geq 150 \mu\text{M}$ ), which suggests the antimicrobial effects may occur from either inhibiting multiple HKs, or by inhibiting off-target enzymes or by damaging effects on the bacterial cell membrane. Given that **5b** and **5c** inhibit both CckA and PhoQ (**Table 2**) *in vitro*, albeit with increased potency for CckA by an order of magnitude, the effects we see on *C. crescentus* may be due to inhibition of multiple HKs. An outstanding question is whether these growth inhibition effects on *C. crescentus* are due to CckA inhibition, and we are currently developing experiments to test this directly. At this time, we cannot rule out that antimicrobial activity occurs from off-target inhibition or from membrane damage.

In summary we report that repurposing diaryl pyrazole-based, ATP-competitive Hsp90 inhibitors as antibiotics targeting HKs is a promising strategy for the development of novel antibacterial agents. We synthesized and evaluated derivatives of CCT018159 and discovered that the presence of a chlororesorcinol ring was the most important structural feature for increasing potency with this series. Inhibitor **5b** demonstrated favorable properties both for biochemical inhibition of CckA, an essential HK in *C. crescentus*, and PhoQ, a HK in *Salmonella* that is essential for virulence, as well as inhibiting growth of three bacterial strains. Interestingly, despite the conservation of the Bergerat fold ATP-binding domain between Hsp90 and HKs, we discovered that not all Hsp90 inhibitors are effective HK inhibitors. This series represents a promising start toward the development of antibiotics that disrupt bacterial signaling pathways. Because these diaryl pyrazole inhibitors also inhibit Hsp90, further development of this series will focus on both increasing the antimicrobial activity and increasing HK inhibition while decreasing Hsp90 inhibition.

## Acknowledgements

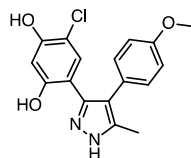
Selected structural analyses were performed with the UCSF Chimera package, which is developed by the Resource for Biocomputing, Visualization, and Informatics at the University of California, San Francisco (supported by NIGMS P41-GM103311). This work was supported in part by Williams College and The Hellman Fellows Fund (J.A.B.). We thank our colleagues Dr. Becky Taurog for her technical support with protein purification and reading of this manuscript, Dr. Nathan Cook for his assistance with NMR and MS analyses, and Prof. Chip Lovett for the *Bacillus subtilis* YB886 strain. We thank Prof. W. Seth Childers, University of Pittsburgh, and members of his lab for the pAP433 plasmid, experimental advice, and thoughtful discussions on this project. We thank Prof. Rui Zhao, University of Colorado, Denver, for plasmid phoQcvt; Prof. Patrick Loll, Drexel University, for vector pETHSUL; and Prof. Gregory Bowman, Washington University School of Medicine, for discussions on molecular docking.

**Table 3.** Hemolysis data against sheep red blood cells and antimicrobial activities against three bacterial strains.

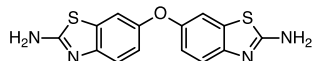
Compound	Hemolysis <sup>a</sup> Mean % hemolysis ± SD	MIC values / $\mu\text{M}$ ( $\mu\text{g mL}^{-1}$ ) <sup>b</sup>		
		<i>E. coli</i> DC2 <sup>76,77</sup>	<i>C. crescentus</i> NA1000 <sup>78</sup>	<i>B. subtilis</i> YB886 <sup>75</sup>
Radicicol	0 ± 1	>300 (>109)	>300 (>109)	>300 (>109)
NVP-AUY922	1 ± 1	37.5–75 (17–35)	>300 (>140)	>300 (>140)
CCT018159	14 ± 10	37.5–75 (13–26)	150–225 (53–79)	112.5 (40)
BIIB 021	6 ± 8	>300 (>95.6)	>300 (>96)	>300 (>96)
PU H71	1 ± 1	75–225 (38–115)	>300 (>154)	>300 (>154)
CUDC-305	3 ± 1	4.7–75 (2–33)	>300 (>133)	>300 (>133)
<b>5a</b>	1 ± 1	37.5–75 (11–23)	225 (68)	150 (45)
<b>5b</b>	3 ± 2	37.5–75 (12–25)	225 (74)	150–225 (50–74)
<b>5c</b>	2 ± 2	75 (27)	225 (81)	112.5–150 (40–54)
<b>5d</b>	2 ± 2	75–150 (22–44)	>300 (>89)	>300 (>89)
<b>5e</b>	15 ± 2	75 (24)	225 (73)	112.5 (36)
<b>7a</b>	0 ± 1	37.5 (11)	150–225 (43–65)	225 (65)
<b>7b</b>	0 ± 1	37.5 (12)	225 (71)	150 (48)
<b>7c</b>	1 ± 1	37.5–75 (13–26)	150–225 (52–78)	112.5–225 (39–78)
<b>7d</b>	3 ± 2	37.5–112.5 (11–32)	>300 (>85)	>300 (>85)

<sup>a</sup> Mean relative hemolysis of citrated sheep red blood cells at 0.5 M compound, 10% (v/v) DMSO, reported as a percentage of the positive control Triton X-100;  $n = 4$ ;  $n = 8$  for the controls; SD = standard deviation.

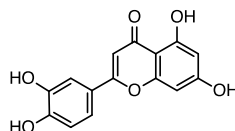
<sup>b</sup> Minimum inhibitory concentration measured using the broth-dilution method; (MIC in  $\mu\text{g mL}^{-1}$  units, calculated from MIC in  $\mu\text{M}$  and MW of each compound);  $n = 2$ –3; ranges indicate the MIC values measured in replicate experiments; concentrations of 300  $\mu\text{M}$  were the highest measured.

**5b**

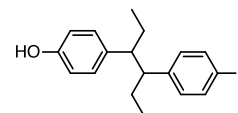
IC<sub>50</sub> *C. crescentus* CckA = 28 μM  
 IC<sub>50</sub> *S. typhimurium* PhoQ = 238 μM  
 IC<sub>50</sub> *C. crescentus* DivJ = no inhibition observed  
 MIC G<sup>+</sup> (*B. subtilis* YB866) = 50–74\* μg mL<sup>-1</sup> (150–225 μM)  
 MIC G<sup>-</sup> (*E. coli* DC2) = 12–25\* μg mL<sup>-1</sup> (37.5–75 μM)  
 MIC G<sup>-</sup> (*C. crescentus* NA1000) = 74\* μg mL<sup>-1</sup> (225 μM)

**Wilke 11**

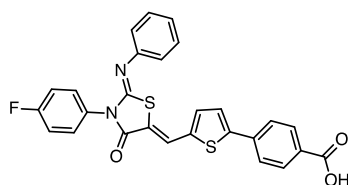
IC<sub>50</sub> *T. maritima* HK853 = 1.21 μM  
 IC<sub>50</sub> *S. pneumoniae* VicK (YycG) = 75 μM  
 IC<sub>50</sub> *E. coli* CheA = no inhibition observed  
 MIC G<sup>+</sup> (*B. subtilis* 3610) = 49–64 μg mL<sup>-1</sup> (156–204\* μM)  
 MIC G<sup>-</sup> (*E. coli* DC2) = 32–64 μg mL<sup>-1</sup> (102–204\* μM)

**Wilke 15 (luteolin)**

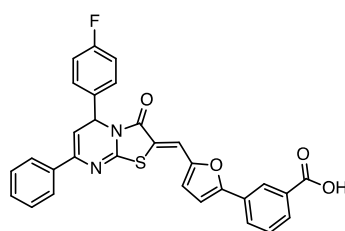
IC<sub>50</sub> *T. maritima* HK853 = 15.1 μM  
 IC<sub>50</sub> *S. pneumoniae* VicK (YycG) = 216 μM  
 IC<sub>50</sub> *E. coli* CheA = 111 μM  
 MIC G<sup>+</sup> (*B. subtilis* 3610) = >128 μg mL<sup>-1</sup> (>447\* μM)  
 MIC G<sup>-</sup> (*E. coli* DC2) = 8 μg mL<sup>-1</sup> (28\* μM)

**Velikova S1.13**

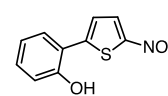
IC<sub>50</sub> *S. aureus* PhoR = 212 μM  
 IC<sub>50</sub> *E. coli* PhoR = 16 μM  
 MIC G<sup>+</sup> (*S. aureus* 20231) = 8 μg mL<sup>-1</sup> (29\* μM)  
 MIC G<sup>-</sup> (*E. coli* CFT073) = >500 μg mL<sup>-1</sup> (1840\* μM)

**Liu H2-81**

IC<sub>50</sub> *S. epidermidis* YycG = 24 μM  
 MIC G<sup>+</sup> (*S. epidermidis* 35984) = 0.75\* μg mL<sup>-1</sup> (1.5 μM)

**Lv H5-33**

IC<sub>50</sub> *S. epidermidis* YycG = 24 μM  
 MIC G<sup>+</sup> (*S. epidermidis* 35984) = 1.6\* μg mL<sup>-1</sup> (3.1 μM)

**Boibessot 6d**

IC<sub>50</sub> *B. subtilis* Walk (YycG) = 197 μM  
 IC<sub>50</sub> *B. subtilis* PhoR = 123 μM  
 IC<sub>50</sub> *B. subtilis* ResE = 124 μM  
 MIC G<sup>+</sup> (*B. subtilis* JH642) = 7 μg mL<sup>-1</sup> (32\* μM)  
 MIC G<sup>-</sup> (*E. coli* MG1655) = 32 μg mL<sup>-1</sup> (145\* μM)

**Figure 6.** Comparison of **5b** to previously reported HK inhibitors. Structures of HK inhibitors with selected biochemical and biological data from earlier studies are shown, and compound names include the lead author surname and the compound name from each study (Boibessot<sup>8</sup>, Lv<sup>14</sup>, Liu<sup>15</sup>, Velikova<sup>17</sup>, Wilke<sup>19</sup>). G<sup>+</sup> = Gram positive strain; G<sup>-</sup> = Gram negative strain. MIC values in each study were reported either in units of μg mL<sup>-1</sup> or μM. For ease of comparison, we calculated each corresponding value using the compound MW, and we denoted (\*) these calculated values.

## References

- Guarnieri MT, Zhang L, Shen J, Zhao R. The Hsp90 inhibitor radicicol interacts with the ATP-binding pocket of bacterial sensor kinase PhoQ. *J Mol Biol.* 2008;379(1): 82-93.
- Silver LL. Challenges of antibacterial discovery. *Clin Microbiol Rev.* 2011;24(1): 71-109.
- Meng EC, Pettersen EF, Couch GS, Huang CC, Ferrin TE. Tools for integrated sequence-structure analysis with UCSF Chimera. *BMC Bioinformatics.* 2006;7(1): 339.
- Pettersen EF, Goddard TD, Huang CC, et al. UCSF Chimera--a visualization system for exploratory research and analysis. *J Comput Chem.* 2004;25(13): 1605-1612.
- Dubey BN, Lori C, Ozaki S, et al. Cyclic di-GMP mediates a histidine kinase/phosphatase switch by noncovalent domain cross-linking. *Sci Adv.* 2016;2(9): e1600823-e1600823.
- Marina A, Mott C, Auyzenberg A, Hendrickson WA, Waldburger CD. Structural and mutational analysis of the PhoQ histidine kinase catalytic domain. Insight into the reaction mechanism. *J Biol Chem.* 2001;276(44): 41182-41190.
- Guarnieri MT, Blagg BSJ, Zhao R. A High-Throughput TNP-ATP Displacement Assay for Screening Inhibitors of ATP-Binding in Bacterial Histidine Kinases. *Assay Drug Dev Technol.* 2011;9(2): 174-183.
- Boibessot T, Zschiedrich CP, Lebeau A, et al. The Rational Design, Synthesis, and Antimicrobial Properties of Thiophene Derivatives That Inhibit Bacterial Histidine Kinases. *J Med Chem.* 2016;59(19): 8830-8847.
- Bruncko M, Tahir SK, Song X, et al. N-aryl-benzimidazolones as novel small molecule HSP90 inhibitors. *Bioorg Med Chem Lett.* 2010;20(24): 7503-7506.

10. Laxminarayan R, Duse A, Wattal C, et al. Antibiotic resistance-the need for global solutions. *Lancet Infect Dis*. 2013;13(12): 1057-1098.
11. Prodromou C, Roe SM, O'Brien R, Ladbury JE, Piper PW, Pearl LH. Identification and structural characterization of the ATP/ADP-binding site in the Hsp90 molecular chaperone. *Cell*. 1997;90(1): 65-75.
12. Wilke KE, Carlson EE. All signals lost. *Sci Transl Med*. 2013;5(203): 203ps212-203ps212.
13. Bem AE, Velikova N, Pellicer MT, Baarlen Pv, Marina A, Wells JM. Bacterial histidine kinases as novel antibacterial drug targets. *ACS Chem Biol*. 2015;10(1): 213-224.
14. Lv Z, Zhao D, Chang J, et al. Anti-bacterial and Anti-biofilm Evaluation of Thiazolopyrimidinone Derivatives Targeting the Histidine Kinase YycG Protein of *Staphylococcus epidermidis*. *Front Microbiol*. 2017;8: 6293.
15. Liu H, Zhao D, Chang J, et al. Efficacy of novel antibacterial compounds targeting histidine kinase YycG protein. *Appl Microbiol Biotechnol*. 2014;98(13): 6003-6013.
16. Stock AM, Robinson VL, Goudreau PN. Two-component signal transduction. *Annu Rev Biochem*. 2000;69: 183-215.
17. Velikova N, Fulle S, Manso AS, et al. Putative histidine kinase inhibitors with antibacterial effect against multi-drug resistant clinical isolates identified by in vitro and in silico screens. *Sci Rep*. 2016;6: 26085.
18. Gotoh Y, Eguchi Y, Watanabe T, Okamoto S, Doi A, Utsumi R. Two-component signal transduction as potential drug targets in pathogenic bacteria. *Curr Opin Microbiol*. 2010;13(2): 232-239.
19. Wilke KE, Francis S, Carlson EE. Inactivation of multiple bacterial histidine kinases by targeting the ATP-binding domain. *ACS Chem Biol*. 2015;10(1): 328-335.
20. Martin PK, Li T, Sun D, Biek DP, Schmid MB. Role in cell permeability of an essential two-component system in *Staphylococcus aureus*. *J Bacteriol*. 1999;181(12): 3666-3673.
21. Jacobs C, Domian IJ, Maddock JR, Shapiro L. Cell cycle-dependent polar localization of an essential bacterial histidine kinase that controls DNA replication and cell division. *Cell*. 1999;97(1): 111-120.
22. Gao R, Stock AM. Biological insights from structures of two-component proteins. *Annu Rev Microbiol*. 2009;63(1): 133-154.
23. Velikova N, Mas N, Miguel-Romero L, et al. Broadening the antibacterial spectrum of histidine kinase autophosphorylation inhibitors via the use of  $\epsilon$ -poly-L-lysine capped mesoporous silica-based nanoparticles. *Nanomedicine*. 2017;13(2): 569-581.
24. Dutta R, Inouye M. GHKL, an emergent ATPase/kinase superfamily. *Trends Biochem Sci*. 2000;25(1): 24-28.
25. Bhat R, Tummalapalli SR, Rotella DP. Progress in the discovery and development of heat shock protein 90 (Hsp90) inhibitors. *J Med Chem*. 2014;57(21): 8718-8728.
26. Shrestha L, Bolaender A, Patel HJ, Taldone T. Heat Shock Protein (HSP) Drug Discovery and Development: Targeting Heat Shock Proteins in Disease. *Curr Top Med Chem*. 2016;16(25): 2753-2764.
27. Wang M, Shen A, Zhang C, et al. Development of Heat Shock Protein (Hsp90) Inhibitors To Combat Resistance to Tyrosine Kinase Inhibitors through Hsp90-Kinase Interactions. *J Med Chem*. 2016: acs.jmedchem.5b01106.
28. Brough PA, Aherne W, Barril X, et al. 4,5-diarylisoaxazole Hsp90 chaperone inhibitors: potential therapeutic agents for the treatment of cancer. *J Med Chem*. 2008;51(2): 196-218.
29. Cheung K-MJ, Matthews TP, James K, et al. The identification, synthesis, protein crystal structure and in vitro biochemical evaluation of a new 3,4-diarylpyrazole class of Hsp90 inhibitors. *Bioorg Med Chem Lett*. 2005;15(14): 3338-3343.
30. Kasibhatla SR, Hong K, Biamonte MA, et al. Rationally designed high-affinity 2-amino-6-halopurine heat shock protein 90 inhibitors that exhibit potent antitumor activity. *J Med Chem*. 2007;50(12): 2767-2778.
31. He H, Zatorska D, Kim J, et al. Identification of potent water soluble purine-scaffold inhibitors of the heat shock protein 90. *J Med Chem*. 2006;49(1): 381-390.

32. Bao R, Lai C-J, Qu H, et al. CUDC-305, a novel synthetic HSP90 inhibitor with unique pharmacologic properties for cancer therapy. *Clin Cancer Res.* 2009;15(12): 4046-4057.
33. McAdams HH, Shapiro L. The architecture and conservation pattern of whole-cell control circuitry. *J Mol Biol.* 2011;409(1): 28-35.
34. Purcell EB, Boutte CC, Crosson S. Two-component signaling systems and cell cycle control in *Caulobacter crescentus*. *Adv Exp Med Biol.* 2008;631: 122-130.
35. Christen B, Abeliuk E, Collier JM, et al. The essential genome of a bacterium. *Mol Syst Biol.* 2011;7: 528.
36. Jacobs C, Ausmees N, Cordwell SJ, Shapiro L, Laub MT. Functions of the CckA histidine kinase in *Caulobacter* cell cycle control. *Mol Microbiol.* 2003;47(5): 1279-1290.
37. Skerker JM, Prasol MS, Perchuk BS, Biondi EG, Laub MT. Two-Component Signal Transduction Pathways Regulating Growth and Cell Cycle Progression in a Bacterium: A System-Level Analysis. *PLoS Biol.* 2005;3(10): e334.
38. Brill M, Fondi M, Fani R, et al. The diversity and evolution of cell cycle regulation in alpha-proteobacteria: a comparative genomic analysis. *BMC Syst Biol.* 2010;4: 52.
39. Kim J, Heindl JE, Fuqua C. Coordination of division and development influences complex multicellular behavior in *Agrobacterium tumefaciens*. *PLoS ONE.* 2013;8(2): e56682.
40. Willett JW, Herrou J, Briegel A, Rotskoff G, Crosson S. Structural asymmetry in a conserved signaling system that regulates division, replication, and virulence of an intracellular pathogen. *Proc Natl Acad Sci U S A.* 2015;112(28): E3709-3718.
41. Ericsson UB, Hallberg BM, DeTitta GT, Dekker N, Nordlund P. Thermofluor-based high-throughput stability optimization of proteins for structural studies. *Anal Biochem.* 2006;357(2): 289-298.
42. Niesen FH, Berglund H, Vedadi M. The use of differential scanning fluorimetry to detect ligand interactions that promote protein stability. *Nat Protoc.* 2007;2(9): 2212-2221.
43. Pantoliano MW, Petrella EC, Kwasnoski JD, et al. High-density miniaturized thermal shift assays as a general strategy for drug discovery. *J Biomol Screen.* 2001;6(6): 429-440.
44. Boivin S, Kozak S, Meijers R. Optimization of protein purification and characterization using Thermofluor screens. *Protein Expr Purif.* 2013;91(2): 192-206.
45. Ji Q, Chen PJ, Qin G, et al. Structure and mechanism of the essential two-component signal-transduction system WalkR in *Staphylococcus aureus*. *Nature Commun.* 2016;7: 11000.
46. Monk IR, Howden BP, Seemann T, Stinear TP. Correspondence: Spontaneous secondary mutations confound analysis of the essential two-component system WalkR in *Staphylococcus aureus*. *Nature Commun.* 2017;8: 14403.
47. McKellar JLO, Minnell JJ, Gerth ML. A high-throughput screen for ligand binding reveals the specificities of three amino acid chemoreceptors from *Pseudomonas syringae* pv. *actinidiae*. *Mol Microbiol.* 2015;96(4): 694-707.
48. Lori C, Ozaki S, Steiner S, et al. Cyclic di-GMP acts as a cell cycle oscillator to drive chromosome replication. *Nature.* 2015;523(7559): 236-239.
49. Mann TH, Seth Childers W, Blair JA, Eckart MR, Shapiro L. A cell cycle kinase with tandem sensory PAS domains integrates cell fate cues. *Nature Commun.* 2016;7: 11454.
50. Chen YE, Tsokos CG, Biondi EG, Perchuk BS, Laub MT. Dynamics of two Phosphorelays controlling cell cycle progression in *Caulobacter crescentus*. *J Bacteriol.* 2009;191(24): 7417-7429.
51. Blair JA, Xu Q, Childers WS, et al. Branched signal wiring of an essential bacterial cell-cycle phosphotransfer protein. *Structure.* 2013;21(9): 1590-1601.
52. Kiiianitsa K, Solinger JA, Heyer WD. NADH-coupled microplate photometric assay for kinetic studies of ATP-hydrolyzing enzymes with low and high specific activities. *Anal Biochem.* 2003;321(2): 266-271.

53. Drysdale MJ, Dymock BW, Barril-Alonso X, et al. 3,4-diarylpyrazoles and their use in the therapy of cancer. U.S. Patent 7 247 734; 2007.
54. Dymock BW, Barril X, Brough PA, et al. Novel, potent small-molecule inhibitors of the molecular chaperone Hsp90 discovered through structure-based design. *J Med Chem.* 2005;48(13): 4212-4215.
55. Sharp SY, Boxall K, Rowlands M, et al. In vitro biological characterization of a novel, synthetic diaryl pyrazole resorcinol class of heat shock protein 90 inhibitors. *Cancer Res.* 2007;67(5): 2206-2216.
56. Howes R, Barril X, Dymock BW, et al. A fluorescence polarization assay for inhibitors of Hsp90. *Anal Biochem.* 2006;350(2): 202-213.
57. Balasubramanian S, Nair MG. An Efficient "One Pot" Synthesis of Isoflavones. *Synth Commun.* 2000;30(3): 469-484.
58. Groisman EA. The pleiotropic two-component regulatory system PhoP-PhoQ. *J Bacteriol.* 2001;183(6): 1835-1842.
59. Miller SI, Kukral AM, Mekalanos JJ. A two-component regulatory system (phoP phoQ) controls *Salmonella typhimurium* virulence. *Proc Natl Acad Sci USA.* 1989;86(13): 5054-5058.
60. Curtis PD, Brun YV. Getting in the loop: regulation of development in *Caulobacter crescentus*. *Microbiol Mol Biol Rev.* 2010;74(1): 13-41.
61. Ohta N, Lane T, Ninfa EG, Sommer JM, Newton A. A histidine protein kinase homologue required for regulation of bacterial cell division and differentiation. *Proc Natl Acad Sci USA.* 1992;89(21): 10297-10301.
62. Grebe TW, Stock JB. The histidine protein kinase superfamily. *Adv Microb Physiol.* 1999;41: 139-227.
63. Francis S, Wilke KE, Brown DE, Carlson EE. Mechanistic insight into inhibition of two-component system signaling. *MedChemComm.* 2013;4(1): 269-277.
64. Bilwes AM, Quezada CM, Croal LR, Crane BR, Simon MI. Nucleotide binding by the histidine kinase CheA. *Nat Struct Biol.* 2001;8(4): 353-360.
65. Perez AM, Mann TH, Lasker K, Ahrens DG, Eckart MR, Shapiro L. A Localized Complex of Two Protein Oligomers Controls the Orientation of Cell Polarity. *mBio.* 2017;8(1): e02238-02216.
66. Weeks SD, Drinker M, Loll PJ. Ligation independent cloning vectors for expression of SUMO fusions. *Protein Expr Purif.* 2007;53(1): 40-50.
67. Shoichet BK. Interpreting steep dose-response curves in early inhibitor discovery. *J Med Chem.* 2006;49(25): 7274-7277.
68. Stephenson K, Yamaguchi Y, Hoch JA. The mechanism of action of inhibitors of bacterial two-component signal transduction systems. *J Biol Chem.* 2000;275(49): 38900-38904.
69. McGovern SL, Caselli E, Grigorieff N, Shoichet BK. A common mechanism underlying promiscuous inhibitors from virtual and high-throughput screening. *J Med Chem.* 2002;45(8): 1712-1722.
70. Hilliard JJ, Goldschmidt RM, Licata L, Baum EZ, Bush K. Multiple mechanisms of action for inhibitors of histidine protein kinases from bacterial two-component systems. *Antimicrob Agents Chemother.* 1999;43(7): 1693-1699.
71. Copeland RA. *Enzymes : a practical introduction to structure, mechanism, and data analysis.* 2nd ed. New York: Wiley; 2000.
72. OEDOCKING. 3.2.0.2 ed. Santa Fe, NM: OpenEye Scientific Software <http://www.eyesopen.com/>.
73. McGann M. FRED and HYBRID docking performance on standardized datasets. *J Comput Aided Mol Des.* 2012;26(8): 897-906.
74. Wiegand I, Hilpert K, Hancock REW. Agar and broth dilution methods to determine the minimal inhibitory concentration (MIC) of antimicrobial substances. *Nat Protoc.* 2008;3(2): 163-175.
75. Yasbin RE, Fields PI, Andersen BJ. Properties of *Bacillus subtilis* 168 derivatives freed of their natural prophages. *Gene.* 1980;12(1-2): 155-159.

76. Clark D. Novel Antibiotic Hypersensitive Mutants of Escherichia-Coli Genetic-Mapping and Chemical Characterization. *FEMS Microbiol Lett.* 1984;21(2): 189-195.
77. Clark DP. Mutant of Escherichia coli deficient in osmoregulation of periplasmic oligosaccharide synthesis. *J Bacteriol.* 1985;161(3): 1049-1053.
78. Marks ME, Castro-Rojas CM, Teiling C, et al. The genetic basis of laboratory adaptation in *Caulobacter crescentus*. *J Bacteriol.* 2010;192(14): 3678-3688.
79. Trajtenberg F, Graña M, Ruétalo N, Botti H, Buschiazzi A. Structural and enzymatic insights into the ATP binding and autophosphorylation mechanism of a sensor histidine kinase. *J Biol Chem.* 2010;285(32): 24892-24903.
80. Gerdes SY, Scholle MD, Campbell JW, et al. Experimental determination and system level analysis of essential genes in Escherichia coli MG1655. *J Bacteriol.* 2003;185(19): 5673-5684.
81. Yamamoto K, Hirao K, Oshima T, Aiba H, Utsumi R, Ishihama A. Functional characterization in vitro of all two-component signal transduction systems from Escherichia coli. *J Biol Chem.* 2005;280(2): 1448-1456.
82. Fabret C, Hoch JA. A two-component signal transduction system essential for growth of *Bacillus subtilis*: implications for anti-infective therapy. *J Bacteriol.* 1998;180(23): 6375-6383.
83. Kobayashi K, Ehrlich SD, Albertini A, et al. Essential *Bacillus subtilis* genes. *Proc Natl Acad Sci USA.* 2003;100(8): 4678-4683.